Appearance of Low Energy Resonances in CO–*Para*-H_2 Inelastic Collisions

Simon Chefdeville,[1,2] Thierry Stoecklin,[1,2] Astrid Bergeat,[1,2] Kevin M. Hickson,[1,2] Christian Naulin,[1,2] and Michel Costes[1,2,*]

[1]*Université de Bordeaux, Institut des Sciences Moléculaires, F-33400 Talence, France*

[2]*CNRS, UMR 5255, F-33400 Talence, France*

(Received 24 April 2012; published 11 July 2012)

We report on crossed-beam experiments and quantum-mechanical calculations performed on the $CO(j = 0) + H_2(j = 0) \rightarrow CO(j = 1) + H_2(j = 0)$ system. The experimental cross sections determined in the threshold region of the $CO(j = 0 \rightarrow j = 1)$ transition at 3.85 cm^{-1} show resonance structures in good qualitative agreement with the theoretical ones. These results suggest that the potential energy surface which describes the CO-H_2 van der Waals interaction should be reinvestigated for good quantitative agreement.

DOI: 10.1103/PhysRevLett.109.023201 PACS numbers: 34.50.Ez, 34.10.+x, 37.20.+j

Shape resonances, also called orbiting resonances in elastic or inelastic collision processes, are associated with quasibound states trapped behind the centrifugal barrier within the shallow potential well which results from the weak van der Waals interaction of the colliding partners as they approach [1]. They correspond to particular quantum-scattering states, or partial waves, each characterized by a fixed value of total angular momentum J which is conserved throughout the collision. The presence of resonance structures may be revealed by sharp enhancements of the integral cross section when the collision energy of the colliding partners matches the energy of the quasibound states. Whereas resonances of this type have been identified in several elastic collision experiments performed in the 1970s [2–6], they have so far eluded experimental observation for inelastic collision events [1]. Quantum-mechanical (QM) calculations performed on potential energy surfaces (PESs) generated by *ab initio* methods predict rich resonance structures in the threshold regions of rotational transitions for many inelastic collision processes between stable molecules or radicals and molecular hydrogen or helium [7–13]. Their observation relies on high-resolution crossed-beam scattering experiments operating in the vicinity of the cold energy regime where most of these features appear. Arguably, the most promising crossed-beam methods for observing such phenomena would employ slow beams of state-selected molecules prepared by Stark or Zeeman deceleration [13–18]. However, state-selected and decelerated beams need to be coupled with cryogenic cooling for H_2 or He supersonic beams and low beam-intersection angles to obtain the prerequisite low energies [13,16]. Indeed, in a collision experiment between two beams of colliding species sharing a reduced mass μ, with laboratory frame velocities v_1 and v_2 and beam-intersection angle χ, the collision energy in the center-of-mass frame or more precisely the relative translational energy is given by

$$E_T = \tfrac{1}{2}\mu({v_1}^2 + {v_2}^2 - 2v_1 v_2 \cos\chi). \quad (1)$$

The lowest relative translational energies are attained only when both laboratory frame velocities are approximately equal. In this respect, deceleration of a single beam does not suffice.

The $CO(j=0)+H_2(j=0)\rightarrow CO(j=1)+H_2(j=0)$ system is suitable for study by both theoretical and experimental means and is also of paramount importance in the interstellar medium. Molecular hydrogen is by far the most abundant molecule in space, followed by carbon monoxide. The ubiquity of CO in galactic and extragalactic sources makes it an excellent tracer of physical conditions, provided its rates of excitation and relaxation by inelastic collisions with H_2 are precisely known. Previous QM calculations describing CO rotational cooling in the low temperature conditions of the interstellar medium have demonstrated the importance of resonances and their sensitivity to the underlying PES that is utilized [7,8]. Here, we report on the first high-resolution crossed-beam experiments to provide the collision energy dependence of state-to-state integral cross sections (otherwise known as the excitation function) in the vicinity of the cold regime, and the experimental results are compared with those of new QM calculations.

We performed experiments with Eq. (1) in mind: both beam velocities were decreased to the lowest possible matched values while reducing the beam-intersection angle as much as physically possible. We obtained low velocity CO and *para*-H_2 beams from cryogenically cooled Even-Lavie fast-pulsed valves [19] (see Table I). The cooling not only slowed down the beams while enhancing their velocity resolution but also quenched most of the internal-state population to the ground rotational state. A minimal energy $E_T = 5.5$ cm^{-1} was obtained in a recent study of the $S(^1D_2) + H_2(j = 0, 1) \rightarrow SH + H$ reaction [20] and $E_T = 9.8$ cm^{-1} when utilizing a neat *para*-$H_2(j = 0)$ beam [21] in an apparatus designed with a minimum intersection angle $\chi = 22.5^\circ$. For the present study, the apparatus was upgraded to attain $\chi = 12.5°$, allowing energies below the threshold of the $CO(j = 0 \rightarrow j = 1)$ rotational transition at

TABLE I. Characteristics of the molecular beams used in the determination of the integral cross sections.

Beam	T^a (K)	v^b (m s^{-1})	δv^c (m s^{-1})	S^d	$\delta\chi^e$ (deg)
CO (1% in He)	75	941.5	24.6	>38	0.9
Para-H_2 (neat)	10	948.4	40.7	>23	2.2

[a]Temperature set point of the cold head. Because no cold shield is used, the effective temperature of the pulsed valve is limited by losses due to thermal radiation. The effective temperature deduced from the beam velocity of a He beam at the lowest set point of the cold head is 35 K higher.

[b]Velocity at the peak. The velocities of the beams are determined from time-of-flight measurements between the crossing point (detection of H_2 or CO by REMPI) and 399 mm downstream with a fast-ionization gauge inserted perpendicular to the molecular beam.

[c]Velocity spread, determined from the broadening of the beam profiles measured as described in note b.

[d]Speed ratio $S \approx v/\delta v_{\mathrm{HWE}}$ (Gaussian limit of the Maxwell-Boltzmann distribution).

[e]Angular divergence (HWE).

3.85 cm^{-1} to be achieved. The CO molecules were detected in the beam crossing region by 2 + 1 resonance-enhanced multiphoton ionization (REMPI) time-of-flight mass spectrometry using two-photon ($E\,^1\Pi$, $v = 0 \leftarrow X\,^1\Sigma_g{}^+$, $v = 0$) transitions around 215.217 nm [22]. The *para*-H_2 beam purity was checked by recording ($C\,^1\Pi_u$, $v = 2 \leftarrow X\,^1\Sigma_g{}^+$, $v = 0$) $R(0)$ and $R(1)$ 3 + 1 REMPI transitions near 289.52 nm, respectively [23], from which a population ratio $j = 0 > 95\%$ was inferred. The spectrum of the CO beam (Fig. 1) recorded around the origin of the ($E\,^1\Pi$, $v = 0 \leftarrow X\,^1\Sigma_g{}^+$, $v = 0$) transition shows a prominent $S(0)$ line surrounded by weak $S(1)$, $R(1)$, and $Q(1)$ lines. The population ratios determined from the intensities of the $S(0)$ and $S(1)$ transitions are 0.99 and 0.01 for $j = 0$ and 1, respectively, corresponding to a rotational temperature $T \approx 1$ K. The excitation functions were obtained with the probe laser tuned to the $Q(1)$ line which is unaffected by the wing of the intense $S(0)$ transition. The residual population of $j = 1$ was subtracted by pulsing the CO beam at 10 Hz

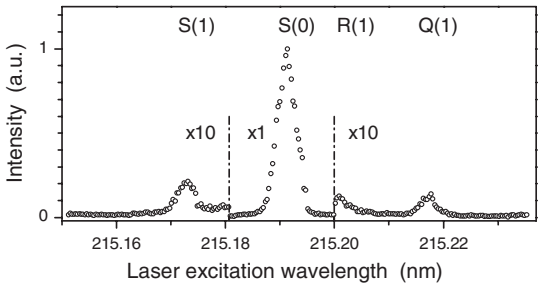

FIG. 1. 2 + 1 REMPI spectrum of the CO($E\,^1\Pi$, $v = 0 \leftarrow X\,^1\Sigma_g{}^+$, $v = 0$) transition. The $S(1)$, $R(1)$, and $Q(1)$ lines are magnified by a factor of 10 for clarity (a.u.: arbitrary units).

and the *para*-H_2 beam at 5 Hz. Cross sections in arbitrary units were directly obtained from the REMPI signal intensities I and the relative velocity v_r of the CO and H_2 beams as $\sigma = I/v_r$. Indeed, the density-to-flux transformation [24] induces negligible corrections because the laboratory frame velocity of the inelastically scattered CO is practically the same as the laboratory frame velocity of the CO beam due to energy and linear momentum conservation. At the highest E_T of 22.5 cm^{-1}, the center-of-mass velocity of CO($j = 1$), $w'_1 = 33$ m s^{-1}, is low compared to $v_1 = 941.5$ m s^{-1}. The integral cross sections displayed in Fig. 2(a) between $E_T = 3.3$ cm^{-1} and 22.5 cm^{-1} result from the accumulation of scans of the beam-intersection angle to reach a statistical uncertainty *ca.* 10% at the 95% confidence interval. This excitation function shows a threshold behavior followed by 3 successive waves α, β, and γ which are clearly the manifestation of resonances. The very sharp rise at the threshold value $E_T = 3.85$ cm^{-1} is the consequence of the low energy spread of the experiment evaluated as δE_T (half-width at $1/e$: HWE) $= 0.077 + 0.051\ E_T - 3.6 \times 10^{-6}\ E_T{}^2$, hence 0.24 cm^{-1} at threshold. Note that the CO($j = 0 \rightarrow j = 2$) transition yields some background signal starting at the threshold value of 11.54 cm^{-1} since the $Q(2)$ line overlaps $Q(1)$ within the laser bandwidth. However, this signal remains negligible due to the lower two-photon transition probability of $Q(2)$ with respect to $Q(1)$ [25].

Second, we performed quantum-mechanical scattering calculations using our diatom-diatom code initially developed for H_2 + HF collisions [26] and the CO-H_2 *ab initio* PES determined by Jankowski and Szalewicz [27]. This surface is based on a five-dimensional grid of *ab initio* points including the dependence on the H-H separation while the C-O separation was fixed. The authors used the coupled-cluster method with single, double, and noniterative triple excitations. Full close coupling calculations were made using the rigid rotor approximation in the $E_T = 0.1$–50 cm^{-1} energy range with 0.01 cm^{-1} increments. The rotational basis set included $j_{H_2} = 0$ and 2 and $j_{CO} = 0$ to 10. The addition of more closed channels of CO or H_2 was seen to alter the magnitude of the CO($j = 0 \rightarrow j = 1$) cross sections by less than 1%. The highest value of total angular momentum J needed to reach convergence at the highest energies sampled was $J = 19$. The propagation was carried out to a maximum distance of 60 bohr, and convergence was checked as a function of the propagator step. The individual partial wave contributions and the resulting integral cross sections are shown in Fig. 2(b). Many sharp shape resonances are present, as well as the Feshbach resonance corresponding to the opening of the CO($j = 0 \rightarrow j = 2$) channel at 11.54 cm^{-1} which starts to compete with the $0 \rightarrow 1$ transition. The theoretical integral cross sections are further convoluted over the collision energy spread and are presented in Fig. 2(a) alongside the experimental results for a

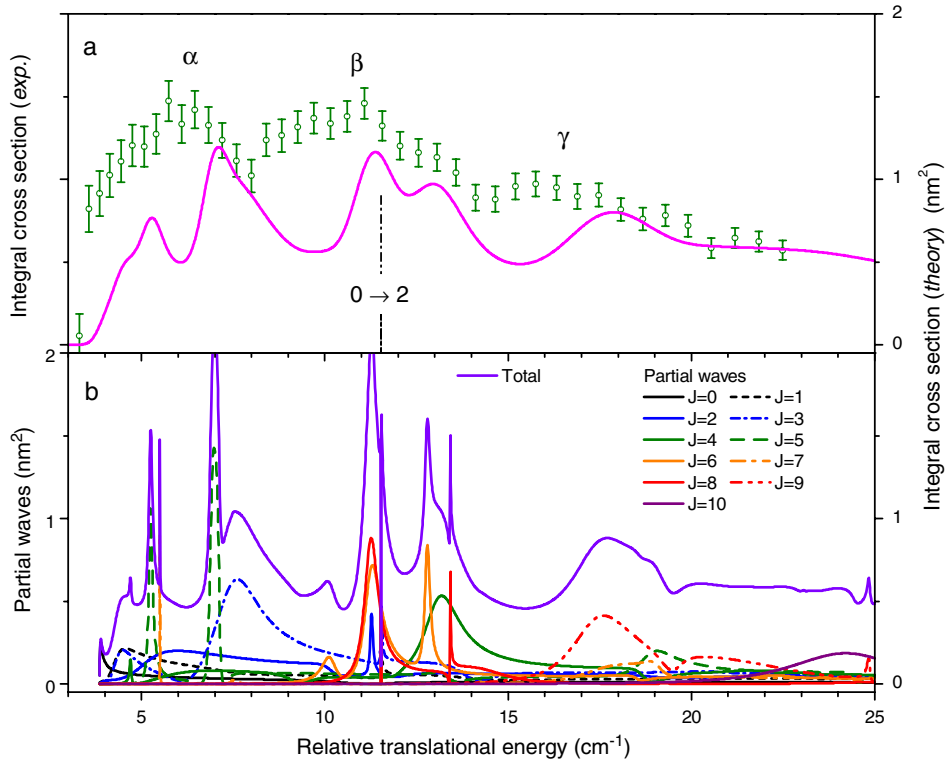

FIG. 2 (color online). (a) Experimental integral cross sections in arbitrary units (open circles with vertical error bars at a 95% confidence interval) and theoretical integral cross sections (solid curve) convoluted over the energy spread. (b) Partial wave cross sections and resulting theoretical integral cross sections from QM calculations performed with the PES of Jankowski and Szalewicz [27].

direct comparison with the experiment. The very sharp features of Fig. 2(b) are smeared out by the energy spread. Nonetheless, three waves persist but with a doubled peak structure for waves α and β and all shifted towards higher energies.

It is well known that resonance features are strikingly dependent on the PES used to perform the QM calculations. A main source of the discrepancy highlighted in Fig. 2(a) could arise from the dissociation energy, D_0, of the CO-H_2 complex respective to the ground-state (000) level. Although the PES is recognized to reach spectroscopic accuracy for the infrared spectrum and the energy levels of the complex, within 0.1 cm^{-1} on average, it yields $D_0 = 19.5$ cm^{-1}, whereas infrared spectroscopic results converge towards $D_0 = 22$ cm^{-1} [28]. The manifold of quasibound states trapped behind the centrifugal barrier and screened by the variation of the relative translational energy near the CO($j = 0 \rightarrow j = 1$) threshold could be shifted substantially by this 2.5 cm^{-1} difference. In an effort to find an agreement with experiment, we applied various scaling factors $f > 1$ to the PES, resulting in a lowering of the global minimum and a concomitant increase of the dissociation energy. The closest match is found for $f = 1.05$, which yields $D_0 = 21$ cm^{-1}. The results of the QM calculations are presented in Fig. 3, and it can be seen that the resonance pattern is indeed strikingly different. Most of the intense peaks have shifted by *ca.* -1 to -1.5 cm^{-1}, which can be accounted for by the difference in D_0 values between the original and the scaled PES, whereas their shapes and strengths are strongly modified. As a result, the initial doubled peak structure of wave α has disappeared. The position of the three waves is now in reasonable agreement with experiment. It becomes clear that wave α borrows its intensity mainly from partial waves $J = 1$, 2, and 3; wave β from $J = 4$, 6, and 8; and wave γ from $J = 5$, 7, and 9. Nonetheless, an agreement on the respective magnitudes of the 3 waves has not been achieved yet. Interestingly, Jankowski and Szalewicz themselves noticed that their *ab initio* PES furnished better results for comparison with the temperature dependence of experimental second-order virial coefficients when rescaled with a factor $f = 1.042$ [27].

In conclusion, our measurements provide the first sensitive probe of a PES under collision conditions approaching the cold energy regime and the first experimental observation of partial wave resonances appearing in the integral cross sections for an inelastic collision process. It has been necessary to rescale the original *ab initio* PES in order to obtain QM results in agreement with the experiment, despite this initial PES being capable of reproducing infrared transitions and energy levels of the CO-H_2 complex with an overall accuracy of 0.1 cm^{-1}. Clearly, the criteria

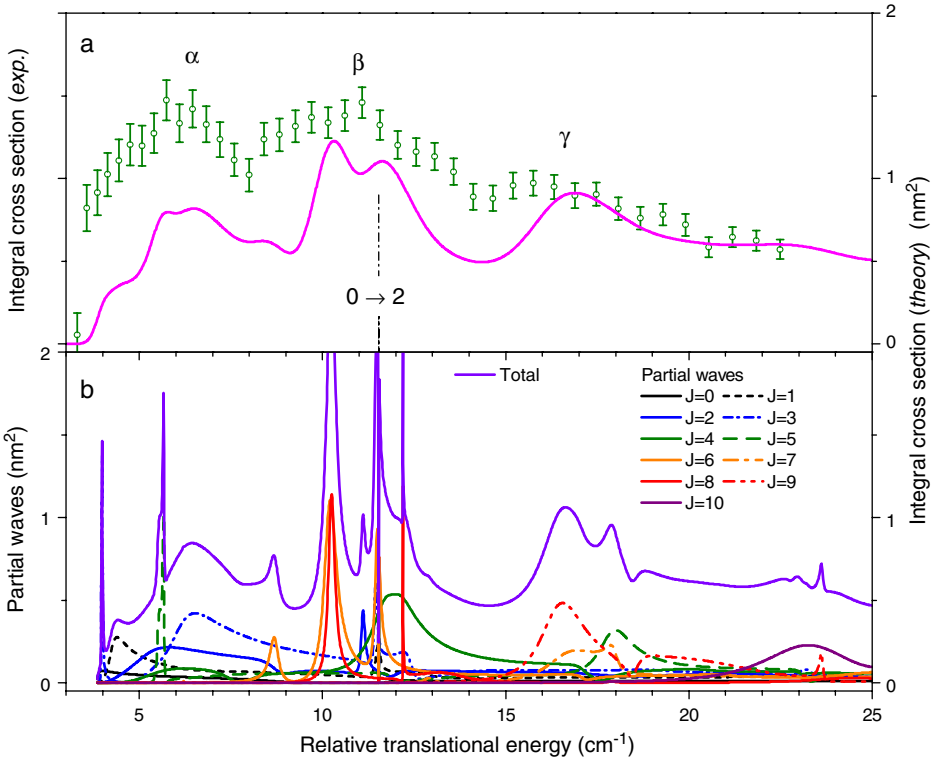

FIG. 3 (color online). (a) Same as Fig. 2(a). (b) Same as Fig. 2(b) with QM calculations performed with the PES of Jankowski and Szalewicz [27] scaled by a factor $f = 1.05$.

demanded by very low energy scattering experiments are even more stringent. In particular, this study shows that a near-perfect representation of the asymptotic region of the PES is of crucial importance.

This work extends the objectives of Contract No. ANR-BLAN-2006-0247 with the Agence Nationale de la Recherche and Contract No. 2007.1221 with the Conseil Régional d'Aquitaine for which financial support is gratefully acknowledged.

*To whom all correspondence should be addressed.
michel.costes@u-bordeaux1.fr

[1] D. W. Chandler, J. Chem. Phys. **132**, 110901 (2010).
[2] A. Schutte, D. Bassi, F. Tommasini, and G. Scoles, Phys. Rev. Lett. **29**, 979 (1972).
[3] A. Schutte, D. Bassi, F. Tommasini, and G. Scoles, J. Chem. Phys. **62**, 600 (1975).
[4] J. R. Grover, J. P. Toennies, W. Welz, and G. Wolf, Chem. Phys. Lett. **48**, 24 (1977).
[5] R. S. Grace, D. L. Johnson, and J. G. Skofronick, J. Chem. Phys. **67**, 2443 (1977).
[6] J. P. Toennies, W. Welz, and G. Wolf, J. Chem. Phys. **71**, 614 (1979).
[7] M. Wernli, P. Valiron, A. Faure, L. Wiesenfeld, P. Jankowski, and K. Szalewicz, Astron. Astrophys. **446**, 367 (2006).
[8] B. Yang, P. C. Stancil, N. Balakrishnan, and R. C. Forrey, Astrophys. J. **718**, 1062 (2010).
[9] Y. Scribano, A. Faure, and L. Wiesenfeld, J. Chem. Phys. **133**, 231105 (2010).
[10] J. Kłos, F. Lique, and M. H. Alexander, Chem. Phys. Lett. **455**, 1 (2008).
[11] F. Lique, A. Spielfiedel, M.-L. Dubernet, and N. Feautrier, J. Chem. Phys. **123**, 134316 (2005).
[12] F. Lique, A. Spielfiedel, N. Feautrier, I. F. Schneider, J. Kłos,, and M. H. Alexander, J. Chem. Phys. **132**, 024303 (2010).
[13] K. B. Gubbels, S. Y. T. van de Meerakker, G. C. Groenenboom, G. Meijer, and A. van der Avoird, J. Chem. Phys. **136**, 074301 (2012).
[14] J. J. Gilijamse, S. Hoekstra, S. Y. T. van de Meerakker, G. C. Groenenboom, and G. Meijer, Science **313**, 1617 (2006).
[15] E. Narevicius, A. Libson, C. G. Parthey, I. Chavez, J. Narevicius, U. Even, and M. G. Raizen, Phys. Rev. Lett. **100**, 093003 (2008).
[16] L. Scharfenberg, S. Y. T. van de Meerakker, and G. Meijer, Phys. Chem. Chem. Phys. **13**, 8448 (2011).
[17] S. D. Hogan, M. Motsch, and F. Merkt, Phys. Chem. Chem. Phys. **13**, 18 705 (2011).
[18] J. H. Blokland, J. Riedel, S. Putzke, B. G. Sartakov, G. C. Groenenboom, and G. Meijer, J. Chem. Phys. **135**, 114201 (2011).
[19] D. Pentlehner, R. Riechers, B. Dick, A. Slenczka, U. Even, N. Lavie, R. Brown, and K. Luria, Rev. Sci. Instrum. **80**, 043302 (2009).

[20] C. Berteloite, M. Lara, A. Bergeat, S. D. Le Picard, F. Dayou, K. M. Hickson, A. Canosa, C. Naulin, J.-M. Launay, I. R. Sims, and M. Costes, Phys. Rev. Lett. **105**, 203201 (2010).
[21] M. Lara, F. Dayou, J.-M. Launay, A. Bergeat, K. M. Hickson, C. Naulin, and M. Costes, Phys. Chem. Chem. Phys. **13**, 8127 (2011).
[22] M. A. Hines, H. A. Michelsen, and R. N. Zare, J. Chem. Phys. **93**, 8557 (1990).
[23] S. T. Pratt, P. M. Dehmer, and J. L. Dehmer, Chem. Phys. Lett. **105**, 28 (1984).
[24] C. Naulin, N. Daugey, K. M. Hickson, and M. Costes, J. Phys. Chem. A **113**, 14 447 (2009).
[25] J. B. Halpern, H. Zacharias, and R. Wallenstein, J. Mol. Spectrosc. **79**, 1 (1980).
[26] G. Guillon, T. Stoecklin, A. Voronin, and P. Halvick, J. Chem. Phys. **129**, 104308 (2008).
[27] P. Jankowski and K. Szalewicz, J. Chem. Phys. **123**, 104301 (2005).
[28] A. R. W. McKellar, J. Chem. Phys. **108**, 1811 (1998).